

## ON THE FORMATION OF PONIUM\*

J. KULPA\*\* AND S. WYCECH†

Sołtan Institute for Nuclear Studies  
Hoża 69, PL-00-681, Warsaw, Poland*(Received January 29, 1996)**Dedicated to Wojciech Królikowski in honour of his 70th birthday*

Some properties of ponium are studied. The decay width in the 1s state is related to the scattering lengths. Chances to produce ponium in hadron-hadron collisions are calculated. Special attention is paid to the effects of an external Coulomb field on the atomic formation process. Corrections to the coalescence model are found and the rate of 2p state production due to the external field is calculated.

PACS numbers: 13.40.Ks, 14.40.-n

## 1. Introduction

The  $\pi\pi$  pair is the simplest two-hadron system. It is expected to be understood in terms of quarks as  $(q\bar{q})(q\bar{q})$ , so the degree of complication is the next after that of a single meson ( $q\bar{q}$ ) or a baryon ( $qqq$ ). At low energies  $\pi\pi$  exhibits also a special approximate symmetry — the chiral symmetry — related to small masses of the quarks. Thus, the  $\pi\pi$  system presents considerable theoretical interest. On the other hand, experimental studies of the  $\pi\pi$  interaction are difficult. There are no pionic targets and one has to resolve final state interactions in  $\pi\pi$  formation processes:

$$\pi N \rightarrow \pi\pi N, \quad \text{or} \quad K \rightarrow \pi\pi e\bar{\nu},$$

which give the  $\pi\pi$  phase shifts only indirectly. We refer the reader to reviews, recent measurements and a compilation [1–3].

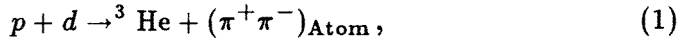
---

\* Work supported by the KBN grant 2p 302 140 04.

\*\* Internet address: JAREKKUL@FUW.EDU.PL

† Internet address: WYCECH@FUW.EDU.PL

A more direct way to learn about the low energy interactions is, in principle, a study of atomic states of the  $\pi^+\pi^-$  pair, called the ponium. The energy levels and, in particular, the lifetimes could give valuable information about the  $\pi\pi$  scattering lengths. So far, the two-meson atomic states have not been experimentally discovered, although, there is some evidence that they are formed in high-energy proton-nucleus collisions [4]. Recently proposals have been made [5, 7] to produce ponium in the reaction



and the experiment has been initiated at the Indiana UCL storage ring. It is mainly this experiment that is discussed here, but the results are easy to extend to the reaction  $pp \rightarrow pp\pi^+\pi^-$  proposed at the COSY-Julich [6], and similar reactions with nuclear targets.

This article presents some known facts: basic features of ponium in Section 2 and the coalescence model used to calculate the rates of atomic formation in some hadron-hadron collisions in Section 3. The new results are given in Section 4 where corrections to the coalescence model are discussed. The latter are due to Coulomb fields of the colliding hadrons. These fields may become a dominant factor in the formation of ponium in the 2p states. Chances for such events are calculated.

## 2. Basic features of ponium

The basic properties of  $\pi^+\pi^-$  atoms are summarized in Table I below.

TABLE I

Bohr radius(fm)	387.46	Width <sub>1s</sub> (eV)	0.24(?)
$E_{1s}$ (keV)	-1.86	Lifetime <sub>1s</sub> ( $10^{-15}$ s)	2.7(?)
$E_{2p}$ (keV)	-0.46	Lifetime <sub>2p</sub> ( $10^{-11}$ s)	0.86
Basic Decay from 1s state	$\pi^0\pi^0$	Decay from 2p state	X-ray

The Bohr radius  $B = 2/(\alpha m_\pi)$  is very large on the scale of strong interactions. Thus the ponium is difficult to produce and easy to destroy. The quantity of special interest is the lifetime linked to the  $\pi^+\pi^-$  scattering length  $A_{cc}$ , as discussed in the Appendix A and given by Eq. (A.8) there. The 1s level width is given by

$$\Gamma = -4\mu^2\alpha^3\text{Im}A_{cc} \quad (2)$$

and  $\text{Im}A_{cc}$  is generated by the isospin symmetry breaking through the meson mass difference  $m(\pi^+) - m(\pi^0)$ . The number given in Table I is uncertain by some 40%. For more details we refer to Appendix A where Eq. (2)

is derived and  $\text{Im}A_{cc}$  is expressed by a combination of the isospin scattering lengths. The lifetime of the atomic 1s-states is too short to be measured directly by electronic methods. The proposed way of measurement [5, 7] is to observe two decay modes:  $\pi^0\pi^0$  and  $\gamma\gamma$ . The former one is by far dominant and determines the decay rate, the latter one is exactly calculable and serves as a reference. One difficulty in using this method is that the coupling to the  $\gamma\gamma$  channel is weak, another one is a large background due to the direct production of  $\pi^0\pi^0$  pairs [12]. One may try to avoid those difficulties by prolongation of the pionium lifetime. This happens when atoms are very fast [4], and/or excited to the 2p-states. The second possibility is discussed in the following Sections.

### 3. The coalescence model

Consider the  $\pi^+\pi^-$  pair produced in a collision of hadrons. Let the transition amplitude be  $F(\vec{P}, \vec{q})$ , where  $\vec{P}$  and  $\vec{q}$  are the total momentum and the relative momentum of the pair. Other quantum numbers needed to specify the collision have been suppressed.

Very little is known on the  $\pi^+\pi^-$  production cross sections in the reactions of interest, and even less is known on the amplitude  $F$ . Nevertheless, the chances to form an atomic state in the final states of the collision may be calculated. It is usually done in a coalescence model. One assumes the formation amplitude  $F_{\text{Atom}}$  to be given by the momentum space atomic wave function  $\tilde{\psi}$

$$F_{\text{Atom}}(\vec{P}) = \int F(\vec{P}, \vec{q}) \tilde{\psi}(\vec{q}) d\vec{q}. \quad (3)$$

Due to the large size of pionium, the momenta involved in  $\tilde{\psi}(\vec{q})$  are very small on the short range scale of the hadronic interactions. Hence, for the atomic s-states

$$F_{\text{Atom}} = F(\vec{P}, \vec{q} = 0) \int \tilde{\psi}(\vec{q}) d\vec{q} = F(\vec{P}, 0) (2\pi)^{3/2} \psi(\vec{r} = 0). \quad (4)$$

Now, this amplitude is given by the atomic wave function at zero range, that is by the normalization factor. This factor is weighted by  $n^{-3/2}$ , where  $n$  is the principal quantum number, and favours the production of 1s state.

One can calculate, quite reliably, the ratio of the atom production to the total pair production  $W_{\text{Atom}}/W_{\text{Total}}$  rates. It is given essentially by the phase space integrals

$$\frac{W_{\text{Atom}}}{W_{\text{Total}}} = \frac{1}{2\mu_{\pi\pi}} |\psi(0)|^2 \frac{\int |F(\vec{P}, \vec{q} = 0)|^2 dL^{k+1}}{\int |F(\vec{P}, \vec{q})|^2 dL^{k+2}}, \quad (5)$$

where  $L^{k+1}$  denotes the phase space for the atom and other  $k$  final state particles. The reduced mass factor  $\mu_{\pi\pi}$  comes from the phase space element, which for a single particle is  $d\vec{p}/[2E(2\pi)^3]$ . A summation over discrete quantum numbers of the other particles is understood. The ratio expected for the reaction (1) close to the threshold is :  $2 \times 10^{-3}$  at  $E_c = E - E_{\text{threshold}} = 1\text{MeV}$ , it decreases to  $8 \times 10^{-5}$  at 10MeV and stabilizes at the level of  $1 \times 10^{-5}$  till 100 MeV, [12]. If the two pion production cross section turns out significant the atomic formation close to or below the  $\pi^+\pi^-$  threshold may be a promising method, [5].

For the  $pp \rightarrow pp\pi^+\pi^-$  reaction the relative rates are similar. Now, the pair production cross section is known. It reaches 100  $\mu\text{b}$  at 100 MeV, and provides at this energy the optimal conditions for the atomic production. At the luminosities of  $10^{32} \text{ cm}^{-2}/\text{s}$  one expects one atom per 100 s. The production rates of this order are large enough for the ponium detection. But, the lifetime in the 1s state is short and difficult to measure. On the other hand, ponium may live longer by orders of magnitude if it is formed in the 2p states. Such a formation would open new experimental possibilities and provide a time scale of  $0.86 \times 10^{-11} \text{ s}$  given by the 2p state lifetime. The latter one is due to the X-ray transitions [8], while other decay modes  $\gamma\gamma\gamma$  and  $e^+e^-$  contribute very little.

In the next Section the chances to form the 2p state atoms are calculated.

### 3.1. The production of atoms in 2p-states

The direct production rate of the 2p states is expected to be slow. As compared to the 1s production rate it involves an additional  $\alpha^2$  factor. The argument is as follows: assume that the  $\pi^+\pi^-$  pair originates from a virtual vector meson (*e.g.*,  $\rho$ ) produced by a reaction such as  $pd \rightarrow \rho^3\text{He}$ . Let the meson production amplitude be  $\vec{\epsilon} \cdot \vec{q}F$ , where  $\vec{\epsilon}$  is a unit vector related to the vector meson. Calculations analogous to those of the previous section yield the branching ratio for the p-wave atom formation

$$\frac{W_{\text{Atom}}}{W_{\text{Total}}} = \frac{3}{8\pi\mu_{\pi\pi}} |\psi'_r(0)|^2 \frac{L^{k+1}}{\langle q^2 L^{k+2} \rangle}. \quad (6)$$

Here,  $\psi'$  is the derivative of the p-wave radial atomic function at zero range ( $\sqrt{(\mu\alpha)^5/24}$  for 2p-state) and  $\langle \cdot \rangle$  is an average of  $q^2$  over the final phase space. Close to the  $\pi^+\pi^-$  production threshold this ratio follows  $E_c^{-5/2}$  and, in principle, may be quite large. In practice the  $\alpha^5$  factor (and the presumably small at these energies vector meson production) make the formation unlikely. Estimates indicate the ratio given by Eq. (6) to be as small as  $10^{-9}$ , [12].

In the next Section another mechanism for the p-wave atom production is introduced. We assume the pair to be produced at short ranges in an s-wave. Subsequent formation of the p-state atoms is achieved by a Stark mixing in the external electric field of the colliding particles .

#### 4. The formation of pionium in external electric fields

In this Section the problem of atomic formation is extended to include the propagation of the  $\pi^+\pi^-$  pairs in an external Coulomb field. The field in question is generated by the colliding hadrons. This is a formidable problem of three-body Coulomb interactions in the continuum. Our special boundary conditions reduce the difficulty but some approximations are still necessary. In particular, we discuss atoms of high velocities *i.e.* close to the coalescent model regime.

The two questions of practical interest are: (1) how does the external field reduce the rate of the dominant 1s-state formation, and (2) what is the fraction of the 2p and higher states generated in this way. A system of successive approximations is developed to answer these questions. Also, a lower limit is obtained for the 1s state formation rate. This calculation shows that the formation of higher atomic states may depend strongly on the total momentum of the pair.

##### 4.1. The formalism

This Section presents our basic assumptions and equations which describe the atom formation. The coalescence model is followed with the assumption that the atom formation amplitude  $F_{\text{Atom}}$  is proportional to the  $\pi\pi$  pair wave function  $\psi$  at zero range

$$F_{\text{Atom}}(P) = F\psi(\vec{q} = 0, \vec{r} = 0, P), \quad (7)$$

where  $F$  is an amplitude of the short range production process. This formula follows Eq. (4) but now  $\psi$  is the pair wave function that contains the atomic state in the asymptotic form and incorporates also the external Coulomb interactions. It depends on the "external" pair centre of mass coordinate  $\vec{q}$ , and the "internal" relative coordinate  $\vec{r}$ . The assumption (7) in  $\vec{r}$  comes from the size of pionium which is much larger than the size of the pair creation region. The condition in  $\vec{q}$  is a dynamic assumption that the  $\pi\pi$  pair at low relative momenta is not likely to come from an intermediate vector meson and is more likely to be produced in an s wave.

The asymptotic form of  $\psi$  consists of an incident wave  $\psi_0$ , and scattered waves  $\psi_{sc}$ . The former is a product of an atomic function  $\varphi_{nl}(r)$ , for the state of interest, and a regular wave in the external coordinate  $q$ . While

the  $\psi_0$  corresponds to the conventional coalescence model the  $\psi_{sc}$  is an effect of the external Coulomb field. As usual, in the description of final state interactions it involves the ingoing partial waves. To calculate this wave an adiabatic situation (*i.e.* slow final state hadrons and fast mesons) is assumed. Such conditions may be fulfilled in the hadronic C.M. system. The external potential  $V$  that generates  $\psi_{sc}$  is

$$V = 2MZ\alpha \left( \frac{1}{|\vec{\varrho} - \frac{\vec{r}}{2}|} - \frac{1}{|\vec{\varrho} + \frac{\vec{r}}{2}|} \right), \quad (8)$$

where  $Z$  is the total charge of the hadrons and  $M = 2m_\pi$ .

The dynamical formation of atomic states of the  $\pi^+\pi^-$  pair is described by the Lippman-Schwinger equation

$$\psi = \psi_0 + \int d^3\varrho d^3r G V \psi. \quad (9)$$

In this equation the problem of the "internal" interactions within the pair have been solved and described by the Green function  $G$ . In principle all the partial waves contribute, but the condition at the origin, Eq. (7), selects only the S waves. Thus, all the internal and external angular momenta are allowed, provided the total angular momentum is zero.

The Green function of the pair  $G$  may be split into a part which contains the internal atomic states  $G^d$  and the rest  $G^c$ . In detail

$$G(\vec{r}, \vec{\varrho}, \vec{r}', \vec{\varrho}') = \sum_{nlm} \varphi_{nlm}(\vec{r}) \varphi_{nlm}^*(\vec{r}') G(\vec{\varrho}, \vec{\varrho}', E - E_n) + G^c, \quad (10)$$

where  $E$  is the total energy of the pair. We are interested in the kinetic energies of the atoms in the 100 keV range (or higher) and neglect the atomic binding energies  $E_n$  (keV range). At first, only the discrete part of the propagator is considered. This allows to expand the wave function in terms of the known internal functions  $\varphi_{nlm}$ , and unknown external functions  $\psi_{nl}(\varrho)$

$$\psi = \sum_{nlm} Y_{lm}(\hat{r}) Y_{lm}^*(\hat{\varrho}) \varphi_{nl}(r) \psi_{nl}(\varrho). \quad (11)$$

Now, the internal degrees of freedom are eliminated by integrating Eq. (9) with  $\varphi_{nl}(r)$  to obtain an infinite set of coupled equations for  $\psi_{nl}(\varrho)$ . These equations involve polarization potentials in the external variable  $\varrho$

$$V_{nln'l'}(\varrho) = \sum_{\lambda=1,3,\dots} \langle \varphi_{nl} | V_\lambda | \varphi_{n'l'} \rangle \Delta(l, l', \lambda), \quad (12)$$

where

$$\Delta(l, l', \lambda) = (2l + 1)(2l' + 1)(2\lambda + 1) \begin{pmatrix} l & l' & \lambda \\ 0 & 0 & 0 \end{pmatrix}^2 \quad (13)$$

which arise from the external potential  $V$  of Eq. (8) in the  $\lambda$ -multipole expansion

$$V(\vec{r}, \vec{\varrho}) = \sum_{\lambda m} V_{\lambda} Y_{\lambda m}^*(\hat{r}) Y_{\lambda m}(\hat{\varrho}), \quad (14)$$

where the dominant role is played by the dipole terms. The latter ones are long-ranged with the  $\varrho^{-2}$  asymptotics and they fall to zero at the origin. Some maxima (or minima) occur at distances comparable to the pionium Bohr radius. There are two main consequences of the long range: one is a Stark-type mixing of the atomic orbits of the propagating pionium, another is a simplicity of the solutions in the high energy region. The latter is discussed in Appendix B, the former is shown in a simple model below.

#### 4.2. An example — two discrete states

An intuitive picture of the formation mechanism is now illustrated with a restricted atomic system which consists of two degenerate states 2s and 2p. These are the states which are coupled most strongly by the polarizing field of Eq. (12). The dipole part of this potential is

$$V_{2p2s}(\varrho) = V_o \frac{(1 + \varrho w)e^{-2\varrho} - 1}{\varrho^2}, \quad (15)$$

where  $V_o = 12\alpha Z m_{\pi}$  is the strength,  $\varrho$  is given in the atomic units and  $w = 2 + 2\varrho + 4/3\varrho^2 + 2/3\varrho^3$  describes the short range cut-off. At distances exceeding the Bohr radius this potential resembles the centrifugal potential of  $\hat{l}^2 = 6Z\alpha$  that for large  $Z$  may be quite strong. At shorter distances it forms a barrier and vanishes at the zero range. In fact, the barrier effect is absent since this is a mixing potential. The solution for  $\psi$  is easy to find numerically and the corresponding atom formation probability is given in Fig. 1 below.

The oscillations of the atomic production probabilities reflect quantum beating in this system. In a strong external electric field there are two orthogonal Stark-states  $s(i)s(e) + p(i)p(e)$  and  $s(i)s(e) - p(i)p(e)$  (here  $s(i), p(e)$  denote the internal and external angular momenta). These two components beat in time and in space when the atom propagates through the polarizing electric field. Condition (7) at the origin selects the s-waves and creates a kind of quantization with respect to  $P$ . An analogy to this effect may be found in the well known oscillations of the  $K_0(\bar{K}_0)$  mesons. Since the long range part of the polarizing potential has no inherent range

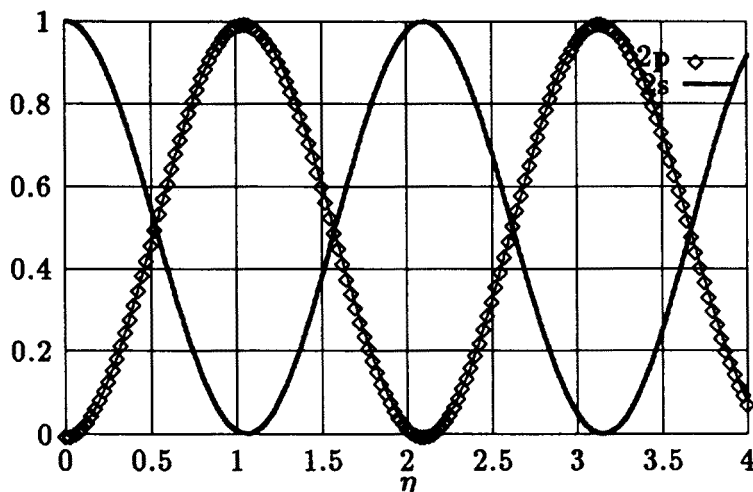


Fig. 1. The probabilities to form ponium in the 2s and 2p states  $W_{2s}$  (continuous line) and  $W_{2p}$  (diamonds). These are calculated in a simple two level model and plotted against the external Coulomb parameter  $\eta = ZM\alpha/P$ . The  $W_{2s}$  is normalized to unity at  $\eta = 0$ .

parameter, the scale in Fig. 1 is given by the dimensionless Coulomb parameter  $\eta = ZM\alpha/P$ . This simple case may be solved exactly. For large total momenta  $P$ , an approximate analytic solution is also possible, it is given in the next Section.

#### 4.3. Solution at high energies

In a more general situation the pair wave functions may be presented in the form

$$\psi_{nl}(\varrho) = j_l(P\varrho)a_{nl}(\varrho) + h_l^-(P\varrho)b_{nl}(\varrho), \quad (16)$$

where  $j_l$  ( $h_l$ ) are the spherical Bessel (Hankel) functions while  $a_{nl}(\varrho)$  and  $b_{nl}(\varrho)$  are to be found. The form of these functions although general has been chosen for the high-energy region which allows approximate solutions. As shown in Appendix B Eqs (B.9)–(B.11) the high energy solutions can be obtained with functions  $a$  changing slowly in space and with  $b \approx 0$ . This property is due to the long range of the polarization potentials. It allows to transform the integral equation (9) to a set of differential equations of the first order

$$a'_{nl} = - \sum_{n'l'} \frac{V_{nl'n'l'}}{2P} a_{n'l'} \sin \left( (l - l') \frac{\pi}{2} \right), \quad (17)$$

where the lengths are expressed in the Bohr radius units.



The equations for  $a_{nl}(\varrho)$  can be written in the following matrix form

$$a' = Ua \quad (18)$$

or  $ia' = iUa$ , where  $U$  is an antisymmetric matrix and respectively  $iU$  is hermitian. The boundary conditions can be formulated via the integral equation

$$a = a_0 + \int_{\varrho}^{\infty} Ua \, d\varrho \quad (19)$$

which is equivalent to the integral equations derived in Appendix B. For example for the incident wave corresponding with the state  $1s$  one has  $a_0 = (1, 0, 0, \dots)$ .

The solutions of Eq. (18) are particularly simple if the matrices  $U(\varrho)$  taken at different values of  $\varrho$  are commuting. This happens at large distances, and there an essential role in the pair propagation is played by eigenvalues of  $U$  which represent some kind of stable Stark-type mixtures of the atomic states. At shorter atomic distances, this simplicity is destroyed by a strong dependence of  $U$  on the atomic quantum numbers.

Now, Eqs (17) are applied to the two-state model of the last Section. To calculate the formation probability of pionium in the  $2s$  state one sets the incident wave  $\psi_0 = \varphi_{2s}(r)j_0(p\varrho)$ . In terms of  $a$ , one has  $a_0 = (1, 0)$  and a simple solution

$$a_{2s}(\varrho) = \cos \left( \frac{1}{2P} \int_{\varrho}^{\infty} V_{2s2p} d\varrho \right) \quad (20)$$

while  $a_{2p}$  is given by the corresponding sine. The atomic formation probability  $W_{2s}(P)$  follows the square of this wave at the origin

$$W_{2s}(P) = W_{2s}(\infty) \cos^2 \left( \frac{1}{2P} \int_0^{\infty} V_{2s2p} d\varrho \right), \quad (21)$$

where  $W_{2s}(\infty)$  is a constant given by the coalescence model. It is a general feature of this calculation that the coalescence model is obtained in the high  $P$  limit.

In order to find the formation probability of pionium in the  $2p$  state one looks for the same function  $a_{2s}(\varrho)$  but with an incident wave  $\psi_0 = \varphi_{2p}(r)j_1(p\varrho)$  or  $a_0 = (0, 1)$ . Now

$$a_{2s}(\varrho) = \sin \left( \frac{1}{2P} \int_{\varrho}^{\infty} V_{2p2s} d\varrho \right), \quad (22)$$

and the probability of the 2P atomic state formation  $W_{2p}(P)$  is

$$W_{2p}(P) = W_{2s}(\infty) \sin^2 \left( \frac{1}{2P} \int_0^\infty V_{2s2p} d\rho \right). \quad (23)$$

The total probability  $W_{2p}(P) + W_{2s}(P)$  is energy independent, and is equal to  $W_{2s}(\infty)$  as a consequence of the flux conservation.

By comparing the analytic results with the numerical solutions one finds the approximation (17) to work well for kinetic energies higher than the barrier in the polarizing potential. In practice it covers the region of the three last peaks in the formation probability. Now the question is, to what extent do the oscillations of the Stark mixed atomic states exist in the complete calculation. The answer is obtained by extension of the basis of the discrete levels allowed in Eq. (11). One result, for the dominant 1s state, is given in Fig. 2. The calculation of  $W_{1s}(P)$  is done with an increasing number of atomic states up to the region when a stable and reasonably precise result is obtained. The beating effect has been lost almost completely although some effect of the 1s - 2p mixing is still visible.

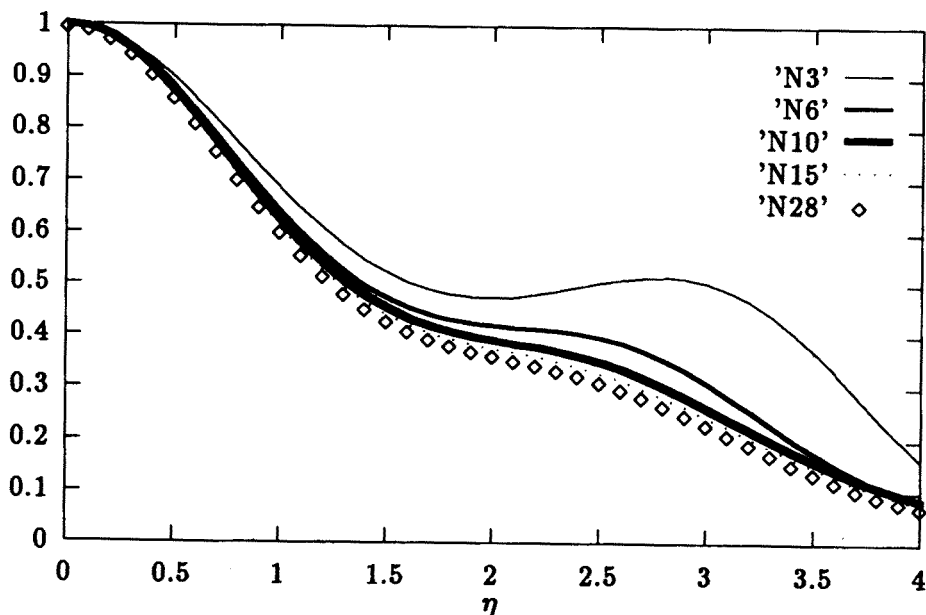


Fig. 2. The probabilities to form 1s atomic state (normalized to the coalescence model value)  $W_{1s}(\eta)/W_{1s}(\eta=0)$  plotted as functions of  $\eta$ . Consecutive curves are calculated with an increasing number of atomic states  $N$ , allowed into the basis of expansion.

The formation probabilities lost in the 1s channel are recovered in the other atomic state channels. The states of prime interest are the 2p states, and the corresponding formation rate is shown in Fig. 3. For some momenta, this rate becomes a sizable fraction of the 1s level formation rate. The rate is high in  $\eta = 2$  region and this corresponds to a maximal mixing effect of the (1s,2p) states. The beating effect of the (2s,2p) components is not noticeable.

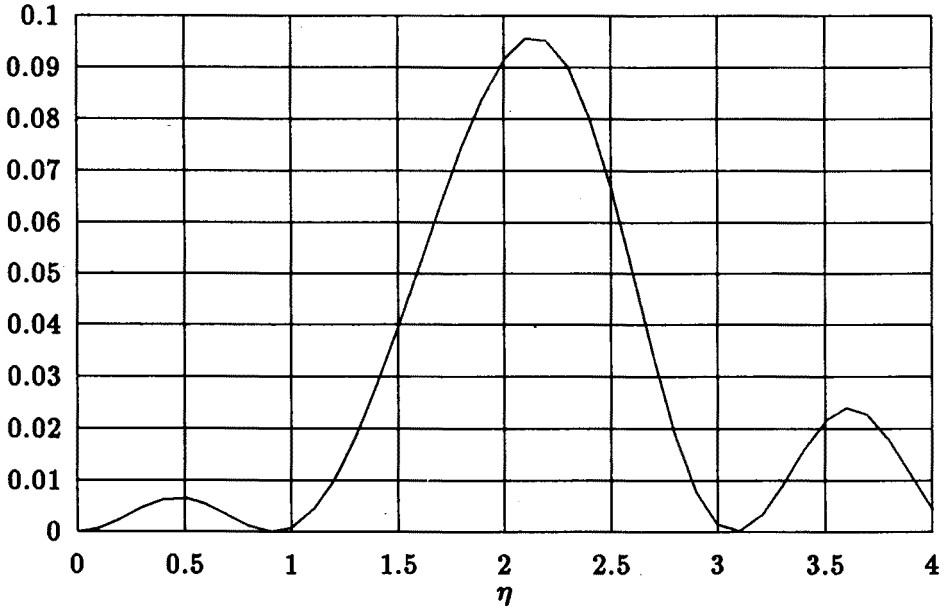


Fig. 3. The probability to form 2p atomic states,  $W_{2p}(\eta)/W_{1s}(\eta=0)$  plotted as a function of  $\eta$ . N=28 states have been used as the basis of expansion.

Within the expansion of Eq. (11), the results given in Fig. 2 and Fig. 3 are fairly reliable. The high energy approximation may be checked against an exact, but limited to several states, calculation. It works for kinetic energies higher than the maxima of the polarization potentials. On the other hand, for higher atomic states the stability and precision of these calculations is less certain. The basis of discrete states must be enlarged and continuum states have to be appended. The solution, even within our approximations, is difficult to obtain.

The role of the internal continuum states is to understand, yet. One effect of these states is an additional destruction of the atomic states. In Appendix C, an upper limit for this destruction is obtained in the case of 1s state formation rate. The high energy approximation and the completeness of internal states make the 1s formation to be unlikely for  $\eta > 1.5$ . Calculations outlined below show that this limit is not reached, however.

The easiest way to find effects of the continuum is to use an optical model type of description. The wave function  $\psi$  is divided into two orthogonal components  $\psi = \psi^d + \psi^c$ , where the first one contains discrete internal states while the other one is composed of the continuum. The same operation is performed with the Coulomb Green function  $G = G^d + G^c$ . Now the Lippman-Schwinger equation is equivalent to a pair of equations for the two parts of  $\psi$

$$\psi^d = \psi_0^d + G^d V \psi^d + G^d V \psi^c, \quad (24)$$

$$\psi^c = G^c V \psi^d + G^c V \psi^c. \quad (25)$$

The interaction within the continuum is not essential, and  $G^c V \psi^c$  is neglected. Next,  $\psi^c$  may be eliminated with the help of Eq. (25) and the equation for  $\psi^d$  follows

$$\psi^d = \psi_0^d + G^d V \psi^d + G^d V G^c V \psi^d. \quad (26)$$

This equation contains an optical potential  $V G^c V$  which involves real and virtual transitions from the atomic to the continuum states  $f_l(kr)$  numbered by momenta  $k$ . The corresponding matrix elements  $\langle f_l(kr) | V | \varphi_{nlm}(r) \rangle$  fall down as  $k^{-3}$  for  $k$  larger than the atomic momenta and cut the high excitations off. This suggests an expansion scheme: one replaces the Coulomb functions  $f_l(kr)$  by any discrete system of orthogonal functions that supplements the atomic wave functions and form a complete basis. The next step is the expansion of  $\psi^c$  in terms of these supplementary functions. Detailed results will be published elsewhere, now we indicate some approximate results. The 1s state formation rate given in Fig. 2 is reduced by about 30 % in the  $\eta > 1.5$  region. The 2p state formation rate given in Fig. 3 remains similar. The maximum of the peak is shifted to  $\eta \approx 1.5$ , however.

This work has a natural extension that may be of interest. In the high  $Z$  situations met in heavy ion collisions the peak in the 2p state formation rate (and similar peaks for higher atomic levels) fall into very high energy region. In particular similar effects are noted for the  $e^+e^-$  pair and the related positonium. The peaks occur in the region of 1.5 MeV of the total energy which is the region of the elusive peaks observed in the  $e^+e^-$  system for  $Z \approx 170$ , [9]. This phenomenon is now being studied with the help of the Krokowski equation for two fermions in an external field, [10].

## 5. Conclusions

The measurement of ponium lifetime may be a source of information on the pion-pion scattering lengths. The rates of ponium production in

hadronic collisions are high enough to observe this system, but experiments that could measure the lifetime in the  $1s$  state are difficult.

In this paper the rates of pionium production in the  $1s$  and  $2p$  states have been calculated. An improvement over the coalescence model is achieved with the inclusion of final state Coulomb interactions. It turns out that the  $p$ -wave states may be formed by the Coulomb field at a rate which is reasonably high for some energies. These states live long and may offer new possibilities for the experimental studies.

## Appendix A

### Scattering parameters

This Appendix provides basic formulas and the parametrization of the low energy scattering in the presence of Coulomb interactions.

Consider  $s$ -wave scattering in a system consisting of two channels  $c$  and  $o$ . The case of special interest is the energy region in-between the thresholds that is a situation when one of the channels  $c$  is closed and the other one  $o$  is open. For phenomenological applications, it is convenient to present the scattering matrix  $\hat{T}$  in terms of a real and symmetric reaction matrix  $\hat{K}$ . These two matrices are related by the Heitler equation  $\hat{T} = \hat{K} - i\hat{K}\hat{q}\hat{T}$  where  $\hat{q}$  is a diagonal matrix of the centre of mass momenta. In a single channel case this equation leads to a natural low energy parametrization  $1/T = 1/a + iq$ , where  $a = K$  is a scattering length related to the phase shift by  $a = -\tan\delta/q$ . A generalization of the scattering length to the many channel situation is provided by the  $\hat{K}$ -matrix. Now, the relation of  $T$  and  $K$  matrices which follows from the Heitler equation is more involved

$$\hat{K} = \begin{pmatrix} K_{oo} & K_{co} \\ K_{oc} & K_{cc} \end{pmatrix} \quad (\text{A.1})$$

and

$$\hat{T} = \begin{pmatrix} T_{oo} & T_{co} \\ T_{oc} & T_{cc} \end{pmatrix} = \begin{pmatrix} \frac{A_{oo}}{1+iq_o A_{oo}} & \frac{A_{co}}{1+iq_c A_{cc}} \\ \frac{A_{oc}}{1+iq_o A_{cc}} & \frac{A_{cc}}{1+iq_c A_{cc}} \end{pmatrix}, \quad (\text{A.2})$$

where  $q_{o,c}$  are the momenta in the two channels  $o, c$  and the channel scattering lengths  $A_{ij}$  are expressed in terms of the  $K$ -matrix elements by [11]

$$\begin{aligned} A_{cc} &= K_{cc} - \frac{iK_{co}^2 q_o}{1 + iq_o K_{oo}}, \\ A_{co} &= \frac{K_{co}}{1 + iq_o K_{oo}}, \\ A_{oo} &= K_{oo} - \frac{iK_{co}^2 q_c}{1 + iq_c K_{cc}}. \end{aligned} \quad (\text{A.3})$$

Notice the unitarity condition, which follows from these equations in the form,

$$\text{Im } A_{cc} = -|A_{co}|^2 q_o. \quad (\text{A.4})$$

These equations form a basis for the description of two channel scattering in terms of the three parameters of the  $K$ -matrix. However, the  $\pi\pi$  systems of interest is believed to display a higher degree of isospin symmetry in their interactions. The  $K$ -matrix may be expressed by two real scattering lengths  $a_0$  and  $a_2$  referring to isospin 0 and 2. The isospin and channel structure  $K$ -matrix is given by : channel  $c$  is  $\pi^+\pi^-$ , channel  $o$  is  $\pi^0\pi^0$  and  $K_{cc} = (a_2 + 2a_0)/3$ ,  $K_{co} = \sqrt{2}(a_2 - a_0)/3$ ,  $K_{oo} = (2a_2 + a_0)/3$ .

The isospin symmetry is broken by Coulomb interactions and meson mass differences. The first allow for atomic binding in the channel  $c$  while the second induce decays of these atomic systems. In this situation the channels are, accordingly, closed ( $c$ ) and open ( $o$ ). To describe the atomic systems in collisions, these effects have to be built into Eqs (A.2), (A.3). The standard way is to put the long range effects into Coulomb propagators  $G^c$  and include the short range effects into "Coulomb corrected" scattering lengths. This separation follows in a natural way the form of the propagator that describes both the Coulomb and the short ranged interactions  $G^c + G^c T G^c$ . As a consequence, the scattering is described by amplitudes of the form

$$f_{ij} = f^c \delta_{ij} + e^{i\sigma} c_i^2 T_{ij}^c c_j^2 e^{i\sigma_j}, \quad (\text{A.5})$$

where  $f^c$ ,  $\sigma$  and  $c^2$  are the Coulomb scattering amplitudes, phases and penetration factors. All these arise as effects of long range Coulomb force. The Coulomb corrections to  $T^c$  arise in terms of short range behaviour of the Coulomb waves. These may be expressed by some functions that should replace  $iq$  in Eqs (A.2), (A.3). Thus, in channel  $c$ :

$$iq \rightarrow f = 2\gamma h + iq c^2, \quad (\text{A.6})$$

$$\text{where } c^2 = \frac{2\pi\eta}{\exp(2\pi\eta) - 1} \quad \text{and} \quad h = \frac{1}{2}[\psi(i\eta) + \psi(-i\eta)] - \frac{1}{2}\ln\eta^2.$$

Also  $\gamma = ZZ'\alpha\mu$  and  $\eta = \gamma/q$ . In the neutral channel  $o$  one has  $f = iq$ . Now, the atomic states created in the intermediate states of nuclear reactions are generated by poles in  $f$  of Eq. (A.6). The singularity of  $f$  has the form

$$f \simeq \frac{R}{E_c - \epsilon_0}, \quad \text{where} \quad R = -\frac{2\pi}{\mu} |\psi(0)|^2 = -2\mu^2 \alpha^3, \quad (\text{A.7})$$

where  $\epsilon_0$  is the pure Coulomb energy of an  $s$ -level and  $E_c$  is the energy relative to the  $\pi^+\pi^-$  threshold.

From Eqs (A.6) and (A.7) one easily finds the position of the atomic pole in  $T_{cc}$  of Eq. (A.2). The atomic level energy is a complex number composed of the Coulomb energy, a level shift due to the strong interactions and an imaginary correction that describes the decay width :

$$\epsilon - \frac{i\Gamma}{2} = \epsilon_0 + \frac{2\pi}{\mu} |\psi(0)|^2 A_{cc} = \epsilon_0 + 2\mu^2 \alpha^3 A_{cc}, \quad (\text{A.8})$$

which is a well known result relating level shifts and widths to the complex scattering length. The width related to  $\text{Im } A_{cc}$  may be expressed by the  $K$ -matrix elements as

$$\frac{\Gamma}{2} = 2\mu^2 \alpha^3 \frac{K_{oc}^2 q_o}{(1 + q_o^2 K_{oo}^2)}. \quad (\text{A.9})$$

The lifetime given in Table I is calculated using  $a_0 = -0.26/m_\pi$   $a_2 = 0.02/m_\pi$  taken from Ref. [3] (note an opposite sign convention). The lengths from Ref. [2] would yield the lifetime longer by 50%.

## Appendix B

### High energy approximation

At high kinetic energies of the pair, the atomic binding energies  $E_n$  may be neglected and the discrete propagator  $G^d$  reduces to the form :

$$G^d(\vec{r}, \vec{\varrho}, \vec{r}', \vec{\varrho}') = \sum_{nlm} \varphi_{nlm}(\vec{r}) \varphi_{nlm}^*(\vec{r}') G(\vec{\varrho}, \vec{\varrho}', E). \quad (\text{B.1})$$

The partial wave expansion

$$G(\vec{\varrho}, \vec{\varrho}', E) = \sum_{lm} g_l(\varrho, \varrho') Y_{lm}^*(\hat{\varrho}) Y_{lm}(\hat{\varrho}') \quad (\text{B.2})$$

with

$$g_l(\varrho, \varrho') = -iP j_l(P\varrho_{<}) h_l(P\varrho_{>}) \quad (\text{B.3})$$

allows us to write the Lippman-Schwinger integral equation (9) as a system of integral equations for the waves  $\psi_{nl}(\varrho)$  of Eq. (11)

$$\psi_{nl}(\varrho) = j_{l_0}(P\varrho) \delta_{nn_0} \delta_{ll_0} + \int g_l(\varrho, \varrho') \sum_{n'l'} V_{nl n'l'} \psi_{n'l}(\varrho'). \quad (\text{B.4})$$

Iterations of these equations involve integrals of smooth, long ranged potentials with the Hankel and Bessel functions. For high momenta  $P$  the latter oscillate rapidly and approximate relations hold :

$$\langle j_l(x)j_{l'}(x) \rangle \approx \frac{1}{2x^2} \cos\left((l-l')\frac{\pi}{2}\right), \quad (\text{B.5})$$

$$\langle n_l(x)n_{l'}(x) \rangle \approx \frac{1}{2x^2} \cos\left((l-l')\frac{\pi}{2}\right), \quad (\text{B.6})$$

$$\langle j_l(x)n_{l'}(x) \rangle \approx \frac{1}{2x^2} \sin\left((l-l')\frac{\pi}{2}\right), \quad (\text{B.7})$$

where  $x = P\rho$  and symbols  $\langle \dots \rangle$  denote mean values of the oscillating functions. When the partial waves  $\psi_{nl}$  are written in the form

$$\psi_{nl} = j_l(P\rho)a_{nl}(\rho) + h_l(P\rho)b_{nl}(\rho) \quad (\text{B.8})$$

and expressions (B.5)–(B.7) are applied, the partial wave equations reduce to

$$a_{nl}(\rho) = \delta_{nn_0}\delta_{ll_0} + \int_{\rho}^{\infty} \frac{1}{2P} \sin\left((l-l')\frac{\pi}{2}\right) \sum_{n'l'} V_{nl n'l'} a_{n'l'}(\rho') d\rho', \quad (\text{B.9})$$

$$b_{nl}(\rho) = \int_0^{\rho} \frac{1}{2P} \sin\left((l-l')\frac{\pi}{2}\right) \sum_{n'l'} V_{nl n'l'} b_{n'l'}(\rho') d\rho'. \quad (\text{B.10})$$

The equations for  $b_{nl}$  are homogeneous and have trivial solutions  $b_{nl} = 0$ . The equations for  $a_{nl}$  are the gateway for the high energy approximation and can be easily written as a system of first order differential equations:

$$a'_{nl} = - \sum_{n'l'} \frac{V_{nl n'l'}}{2P} a_{n'l'} \sin\left((l-l')\frac{\pi}{2}\right). \quad (\text{B.11})$$

These equations may be also obtained in an alternative way as a WKB approximation.

## Appendix C

### *Closure approximation*

In this Section we go one step beyond the high energy approximation of the last Section. Again, the internal energies are neglected in comparison



to the kinetic energy of the atom  $E$ . Now the full internal spectrum is used and that leads to the approximate formula for the propagator

$$G(\vec{r}, \vec{\varrho}, \vec{r}', \vec{\varrho}', E) \approx G(\vec{\varrho}, \vec{\varrho}', E) \delta(\vec{r} - \vec{r}'). \quad (\text{C.1})$$

In this equation  $G(\vec{\varrho}, \vec{\varrho}', E)$  is the one body free Green function of Eq. (B.2) which can be written in terms of partial wave radial propagators (B.3). For high energies and large  $P\varrho$  we have the following properties of  $g_l(\varrho, \varrho')$ :

$$\begin{aligned} g_l &\approx g_0 & \text{for } l \text{ even,} \\ g_l &\approx g_1 & \text{for } l \text{ odd,} \end{aligned} \quad (\text{C.2})$$

that reduce the propagator to

$$\begin{aligned} G(\vec{\varrho}, \vec{\varrho}', E) &= g_0(\varrho, \varrho') \sum_{l-\text{even}, m} Y_{lm}(\hat{\varrho}) Y_{lm}^*(\hat{\varrho}') \\ &+ g_1(\varrho, \varrho') \sum_{l-\text{odd}, m} Y_{lm}(\hat{\varrho}) Y_{lm}^*(\hat{\varrho}') \end{aligned} \quad (\text{C.3})$$

The total angular momentum of the created pairs is zero and the corresponding piece of the total propagator (C.1) is needed. It means that the sum over angular momenta is limited to  $l = l_{\text{internal}}$  and

$$\begin{aligned} G(\vec{r}, \vec{r}', \vec{\varrho}, \vec{\varrho}') &= (g_0(\varrho, \varrho') \sum_{l-\text{even}, m, m'} Y_{lm}(\hat{\varrho}) Y_{lm}^*(\hat{\varrho}') Y_{lm'}(\hat{r}) Y_{lm'}^*(\hat{r}')) \\ &+ g_1(\varrho, \varrho') \sum_{l-\text{odd}, m, m'} Y_{lm}(\hat{\varrho}) Y_{lm}^*(\hat{\varrho}') Y_{lm'}(\hat{r}) Y_{lm'}^*(\hat{r}')) \delta(r - r'). \end{aligned} \quad (\text{C.4})$$

It follows from this approximate form of the propagator that the variable  $r$  is frozen and plays no dynamic role. The polarization potential given by Eq. (8) may be written in terms of  $r$  as well as  $\varrho$  and  $z = \cos \theta(\vec{\varrho}, \vec{r})$

$$V = 2\eta P \left( \frac{1}{\sqrt{\varrho^2 - \varrho r z + r^2/4}} - \frac{1}{\sqrt{\varrho^2 + \varrho r z + r^2/4}} \right).$$

The Lippman-Schwinger equation (9) may be formally solved by iterations. Using the approximate propagator from Eq. (C.4) one obtains the solution

$$\psi = \psi_0 + \hat{g}_1 V \psi_0 + \hat{g}_0 V \hat{g}_1 V \psi_0 + \dots \quad (\text{C.5})$$

In this solution both  $r$  and  $z$  appear as parameters in the polarization potential  $V$  and the wave function  $\psi_0$ . The iterations are now calculated

for the atomic formation of the  $1s$  state and the incident wave is  $\psi_0 = j_0(P\rho)\varphi_{1s}(r)$ . The approximate high energy averages (B.5)–(B.7) of the Bessel functions reduce the series for  $\psi(\rho, r, z)$  to the form

$$\begin{aligned} \psi = & j_0(P\rho)\varphi_{1s}(r) \left( 1 - \frac{1}{(2P)^2} \int_{\rho}^{\infty} d\rho' V \int_{\rho'}^{\infty} d\rho'' V + \dots \right) \\ & - j_1(P\rho)\varphi_{1s}(r) \left( \frac{1}{2P} \int_{\rho}^{\infty} d\rho' V - \frac{1}{(2P)^3} \int_{\rho}^{\infty} d\rho' V \int_{\rho'}^{\infty} d\rho'' V \int_{\rho''}^{\infty} d\rho''' V + \dots \right) \end{aligned} \quad (\text{C.6})$$

In that approximation the solution becomes real and it is easy to find a close expression for the multiple integrals

$$\int_{\rho}^{\infty} d\rho' V \int_{\rho'}^{\infty} d\rho'' V = \frac{1}{2!} \left( \int_{\rho}^{\infty} d\rho V \right)^2, \quad (\text{C.7})$$

$$\int_{\rho}^{\infty} d\rho' V \int_{\rho'}^{\infty} d\rho'' V \int_{\rho''}^{\infty} d\rho''' V = \frac{1}{3!} \left( \int_{\rho}^{\infty} d\rho V \right)^3 \quad (\text{C.8})$$

*etc*, so now we are able to add all terms occurring in equation (C.5)

$$\begin{aligned} \psi(\rho, r, z) = & j_0(P\rho)\varphi_{1s}(r) \cos \left( \frac{1}{2P} \int_{\rho}^{\infty} d\rho V(\rho, r, z) \right) \\ & - j_1(P\rho)\varphi_{1s}(r) \sin \left( \frac{1}{2P} \int_{\rho}^{\infty} d\rho V(\rho, r, z) \right). \end{aligned} \quad (\text{C.9})$$

It is easy to integrate the polarization potential over  $\rho$

$$\int_{\rho}^{\infty} d\rho V(\rho, r, z) = 2MZ\alpha \ln \frac{2\rho - rz + \sqrt{(4\rho^2 + r^2 - 4\rho rz)}}{2\rho + rz + \sqrt{(4\rho^2 + r^2 + 4\rho rz)}}, \quad (\text{C.10})$$

$$\int_0^{\infty} d\rho V(\rho, r, z) = 2MZ\alpha \ln \left( \frac{1-z}{1+z} \right), \quad (\text{C.11})$$

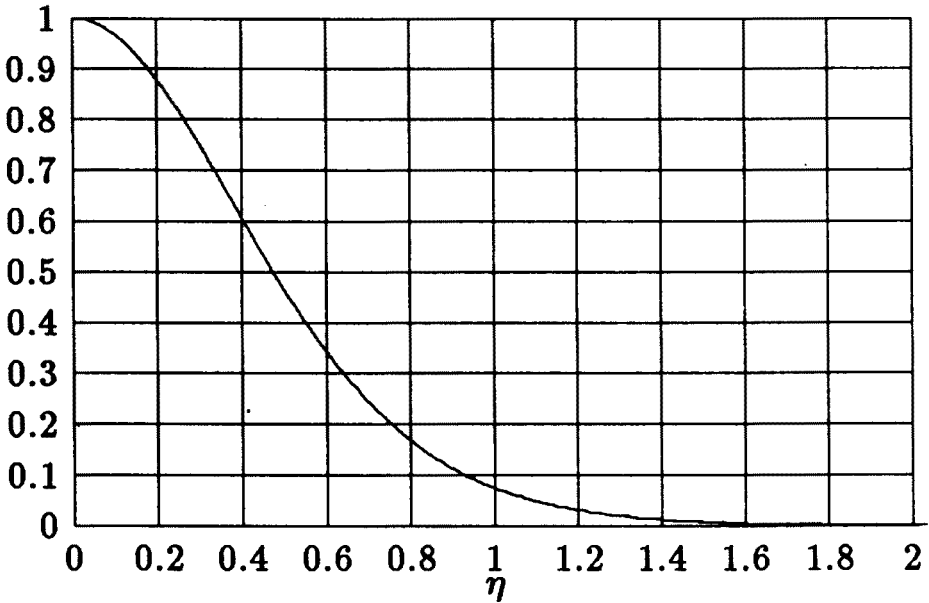


Fig. 4. Probability  $W_1$ , to form pionium in the 1s state calculated in completeness approximation.

and this allows to present the  $l = 0$  component of the the wave function at the zero range

$$\psi(0, 0) = \frac{1}{2} \varphi_{1s}(0) \int_{-1}^1 \cos\left(\eta \ln\left(\frac{1-z}{1+z}\right)\right) dz \quad (\text{C.12})$$

which may be explicitly calculated and reduced to  $\Gamma(1+i\eta)\Gamma(1-i\eta)\varphi_{1s}(0)$ . Finally, the closure approximation formula for the 1s atomic state formation rate becomes

$$|\psi(0, 0)|^2 = \frac{\pi^2 \eta^2}{(\sinh(\pi\eta))^2} \varphi_{1s}(0)^2. \quad (\text{C.13})$$

The energy dependence given by Eq. (C.13) is ruled by the dimensionless Coulomb parameter  $\eta$ . The interpretation is fairly simple: the result is a product of the coalescence formation factor  $\varphi_{1s}(0)^2$  and two penetration factors for the positively and negatively charged particles  $\pi^2 \eta^2 / (\sinh(\pi\eta))^2$ .

## REFERENCES

- [1] B.R. Martin, D. Morgan, G. Shaw, *Pion-Pion Interactions in Particle Physics*, Academic Press 1976; W. Ochs, Results on Low Energy  $\pi\pi$  Scattering, MPI-Ph/Ph 91-35 a contribution to  $\pi N$  News Letter, eds G. Hohler, W. Kluge and B.M.K. Nefkens.
- [2] D. Pocanic *et al.*, *Phys. Rev. Lett* **72**, 1156 (1995).
- [3] O. Dumbrajs *et al.*, *Nucl. Phys.* **216**, 277 (1983).
- [4] L.G. Afanasyev *et al.*, *Phys. Lett.* **B255**, 146 (1991); **B308**, 200 (1993).
- [5] H. Nann, Proc. Workshop on Meson Production, Interaction and Decay, Cracow, Poland May 6-11 1991, eds A. Magiera, W. Oelert and E. Grosse, World Scientific, 1991, p.100; S. Vigdor, Proposal at IUCF.
- [6] W. Oelert, Workshop on Meson Production, Interaction and Decay, Cracow, Poland May 6-11 1991, eds A. Magiera, W. Oelert and E. Grosse, World Scientific, 1991, p.199
- [7] CELSIUS proposal, Meson production in light ion collisions at CELSIUS — spokesmen: B. Höistad and T. Johansson
- [8] O. Dumbrajs, *Z. Phys.* **A321**, 297 (1985).
- [9] P. Salabura *et al.*, *Phys. Rev. Lett.* **56**, 444 (1991).
- [10] W. Krolkowski, *Acta Phys. Pol.* **B25**, 1125 (1994).
- [11] H. Pilkuhn, *The Interaction of Hadrons*, North Holland, 1967, p.207.
- [12] A.M. Green, S. Wycech, *Nucl. Phys.* **A562**, 446 (1993).